frontiers | Frontiers in Earth Science

ORIGINAL RESEARCH
published: 19 April 2022
doi: 10.3389/feart.2022.839995

Seismic Constraints on the Trompsburg Layered Igneous Intrusion Complex in South Africa Using Two Deep Reflection Seismic Profiles

Michael Westgate[1], *Musa S. D. Manzi*[1]*, *Ian James*[2], *Marco A. G. Andreoli*[1,3] *and Raymond J. Durrheim*[1]

[1]School of Geosciences, University of the Witwatersrand, Johannesburg, , South Africa, [2]Southern Geoscience Consultants, West Perth, WA, Australia, [3]Department of Mechanical Engineering Science, University of Johannesburg, Johannesburg, South Africa

The discovery and characterization of layered intrusions around the globe have been predicated to a large degree on the imaging capabilities of the reflection seismic method. The ability of this tool to detect mineralization zones and structural controls such as faults and folds has been critical in unlocking the economic potential of igneous complexes, most notably the Bushveld Complex in South Africa. In this study, we present novel seismic constraints on the lesser-known Trompsburg Complex in South Africa. Two yet-unpublished seismic profiles were conducted end-to-end in the early 1990s, with a southwest-to-northeast trend through the centre of the ~2,400 km^2 Trompsberg potential field anomaly in South Africa, attributed to a 1915 ± 6 Ma buried layered intrusion complex. The complex was first detected by magnetic and gravity measurements near the town of Trompsburg in 1939 and was subsequently confirmed as a layered intrusion by borehole cores drilled thereafter. The combined length of the two profiles is 108 km. Both profiles have been reprocessed and interpreted to further constrain the subsurface expanse of the Trompsberg Complex along the seismic traverse. Processing and interpretation of the seismic profiles were aided by a handful of studies found in the literature: stratigraphy and physical property measurements of borehole cores that were drilled into the complex in the 1940s; pre-Karoo (~317 Ma) lithological maps that were constructed based on boreholes in and around the investigation area; and potential field maps of the intrusion area near the town of Trompsburg. Most of the seismic reflection energy is concentrated within the top 1 km in both profiles, where localized reflectors with strong amplitudes are observed, due likely to the dolerite sills that permeate the Karoo cover. These sills obstruct seismic illumination of underlying structures due to their high acoustic impedance contrast with the surrounding soft rock sediments, rendering underlying reflections challenging to identify and enhance. The base of the Karoo is confidently identified to be at an average depth of 1.5 km and several reflection packages have been identified thereunder. These are linked to Proterozoic supracrustals associated with the Witwatersrand, Ventersdorp, Transvaal/Griqualand West, and Kheis Supergroups, as well as the Trompsburg Complex that intruded into them. The

OPEN ACCESS

Edited by:
Bjarne Sven Gustav Almqvist, Uppsala University, Sweden

Reviewed by:
Craig Magee, University of Leeds, United Kingdom
John McBride, Brigham Young University, United States

***Correspondence:**
Musa S. D. Manzi
musa.manzi@wits.ac.za

Specialty section:
This article was submitted to Solid Earth Geophysics, a section of the journal Frontiers in Earth Science

Received: *20 December 2021*
Accepted: *22 March 2022*
Published: *19 April 2022*

Citation:
Westgate M, Manzi MSD, James I, Andreoli MAG and Durrheim RJ (2022) Seismic Constraints on the Trompsburg Layered Igneous Intrusion Complex in South Africa Using Two Deep Reflection Seismic Profiles. Front. Earth Sci. 10:839995. doi: 10.3389/feart.2022.839995

geometry of the Trompsburg Complex along the seismic traverse has been constrained with a moderate degree of confidence. It comprises a series of 30° northeasterly dipping reflectors near its southwestern boundary, flat reflectors near its centre at the town of Trompsburg, and 45° southwesterly dipping reflectors near its northeastern boundary. The lateral sub-Karoo extent of the complex is 60 km and its total thickness is difficult to constrain due to lack of deep reflections, but is likely between 6.6 and 7.5 km. The complex subcrops against the Karoo cover except near the southwestern region, where it is overlaid by Waterberg Group sediments.

Keywords: reflection, seismic, 2D, Trompsburg complex, hardrock, South Africa

INTRODUCTION

The reflection seismic method has been used extensively for, among others, mineral exploration and hardrock prospection (e.g., Pretorius, 1986; Durrheim, 2015; Manzi et al., 2019; Malehmir et al., 2021). Challenges presented by these environments are related to complex wavefield phenomena, such as scattering and diffraction, which are caused by sharp

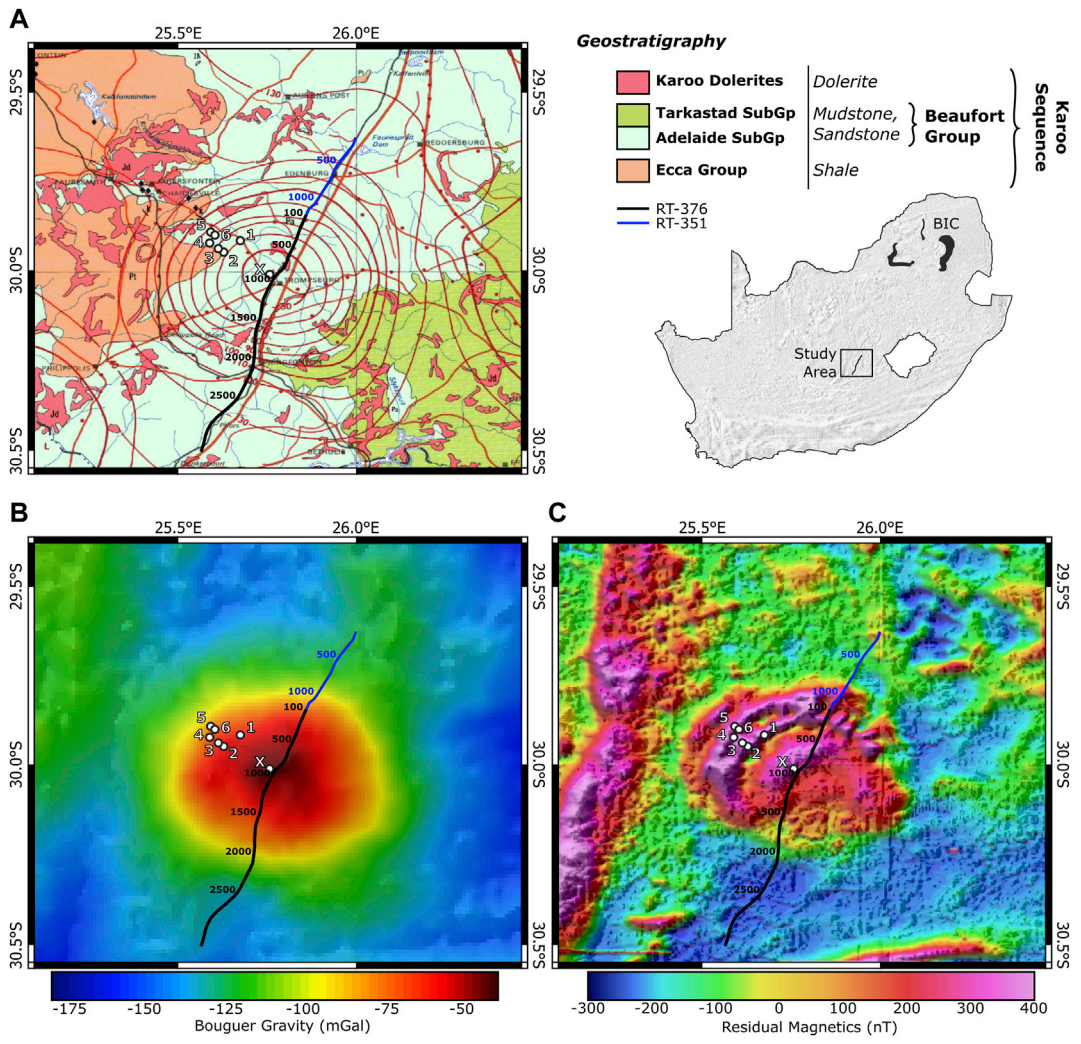

FIGURE 1 | Geological **(A)** and potential field maps, gravity in **(B)** and magnetic in **(C)**, of the Trompsburg anomaly with seismic profiles P1 (RT-376) and P2 (RT-351) overlaid in black and blue, respectively. Profile CMP numbers are labelled every 500th CMP. Boreholes are labelled 1 through 6 in the NW and X in the centre, corresponding to boreholes TG1 through TG6 and TGX, respectively. BIC, Bushveld Igneous Complex.

discontinuities, heterogeneities and anisotropies in the seismic velocity and density fields. Complex layering of rocks, metamorphic scars, and structural constraints that typify the hardrock setting hinder seismic detection and interpretation (Pretorius et al., 2003; Buske et al., 2015). Despite these challenges, the robustness of this method in imaging the subsurface with unprecedented accuracy and resolution renders it exceedingly valuable in the exploration and mining industry. In particular, structural constraints on mineral deposits and host rocks associated with igneous plumbing systems have been successfully mapped using the reflection seismic approach across diverse sets of geological, tectonic, and geomorphological environments (e.g., Scheiber-Enslin and Manzi, 2018; Manzi et al., 2019; Sehoole et al., 2020).

In South Africa, a substantial portion of the world-class gold and platinum deposits were characterized using the reflection seismic method prior to their exploitation. Such projects included the vast amount of corporate-funded seismic surveys that targeted the Bushveld Igneous Complex, the world's largest layered igneous intrusion, now accountable for 90% of the world's platinum group matals (PGM) reserves, as well as its substantial contribution to production of chromite and palladium. In this study, the reflection seismic method is used to image complex lithostratigraphic and structural features of the ~1915 Ma layered igneous intrusion in South Africa called the Trompsburg Complex, named after the town located at its centre (**Figure 1**).

Following the discovery of the positive, 50-km-wide Trompsburg gravity anomaly in 1944 near the town of Trompsburg, South Africa, several efforts were made to investigate the geology lying beneath the overlying sedimentary cover of the Carboniferous to Jurassic Karoo basin. Gravimetric and magnetometric surveys were conducted, followed by the drilling of seven exploration boreholes into the centre and northwestern rim of the geophysical anomaly, where the magnetic map of the anomaly exhibited concentric arcs of high amplitudes (**Figure 1**). The results of these surveys were initially documented by Ortlepp (1959) and Buchmann, (1960), which revealed a series of layered igneous intrusions beneath the Karoo cover, leading both authors to conclude the presence of a buried igneous complex. The former suggested an average total thickness of 3 km for the complex, and the latter a thickness of 10 km. The six boreholes in the northwestern region of the anomaly revealed several layers of mafic intrusions, including gabbros, anorthosite and magnetite, beneath the Karoo sedimentary rocks and dolerite sills, while the borehole near the centre of the anomaly only intersected granite beneath the Karoo.

Significant amounts of magnetite were observed within the layered intrusions, prompting multiple studies into the economic potential of the complex (Logan, 1979; Reynolds, 1979). Such studies revealed strong mineralogical and chemical correlations between the Trompsburg Complex and regions of the Bushveld Igneous Complex, suggesting the former to be a satellite intrusion of the latter (McCarthy et al., 2018). However, Rb-Sr isotopic and zircon dating of core samples from the Trompsburg Complex by Maier et al. (2003) yielded an age of 1915 ± 6 Ma, ~140 Ma younger than the crystallization of the Bushveld Igneous Complex at 2056 ± 4 Ma (cf. Walraven and Hattingh, 1993; Buick et al., 2001), and a derivation from a different, relatively depleted mantle source (Maier et al., 2003). McCarthy et al. (2018) comment on the striking similarity of lithologies between the two complexes and suggest that redating of the Trompsburg Complex should be undertaken.

The first attempt at a 3D model of the Trompsburg Complex was made by Maré and Cole (2006) based on physical property measurements they had conducted on retrieved core from the 1960 exploration boreholes. Density and magnetic susceptibility measurements conducted on the core samples were used to forward model the potential field anomaly of the Trompsburg Complex. Their model comprises an 8-km-thick layered intrusion with an average diameter of 65 km and an 8 km thick central feeder, totaling a thickness of 16 km near the centre of the complex. While the modelled potential field data correlate well with the observed field data, Maré and Cole (2006) Stress the ambiguity of potential field modelling, which in their study was exacerbated by the restriction of constraining borehole data to the centre and NW region of the complex. No further geological or geophysical investigations into the structure of the Trompsburg Complex have been conducted to verify or constrain its three-dimensional extent.

In the late 1980s and early 1990s, AngloGold Ashanti Ltd., then the Gold Division of the Anglo-American Corporation, commissioned several 6 and 16 s 2D seismic profiles to map crustal-scale structures across the Kaapvaal Craton in search of gold-bearing Witwatersrand Supergroup outliers (Durrheim, 2015). Most of these data have been donated to the Seismic Research Centre at the University of the Witwatersrand, South Africa, for crustal and mineralogical research. Since their acquisition, a handful of these profiles have been published in the literature (e.g. Stettler et al., 1999; Tinker et al., 2002; Westgate et al., 2020; Westgate et al., 2021), but many remain unpublished. Amongst the undisclosed surveys are two 6 s profiles that traverse the centre of the Trompsburg Complex with a SW-NE bearing (shown in **Figure 1**), namely profiles RT-376 in the SW and RT-351 in the NE. For simplicity, we refer to profiles RT-376 and RT-351 throughout the rest of this paper as P1 and P2, respectively. We have reprocessed these profiles separately using a standard reflection processing flow to obtain a migrated image of the subsurface that extends to a depth of ~15 km. Our reprocessing and interpretation of the seismic profiles have been informed by the aforementioned borehole and physical property studies, as well as geophysical and geological maps in the literature.

The primary objective of reprocessing the two seismic profiles is to image structural features beneath the Karoo sediments and dolerites that are related to the Trompsburg Complex. Secondary objectives include constraining the Karoo cover thickness and investigating pre-Trompsburg structures beneath the Karoo.

REGIONAL GEOLOGY AND GEOPHYSICS

Seismic profiles P1 and P2 are plotted on surface geology, gravity, and magnetic maps in **Figure 1**. The Trompsburg Complex

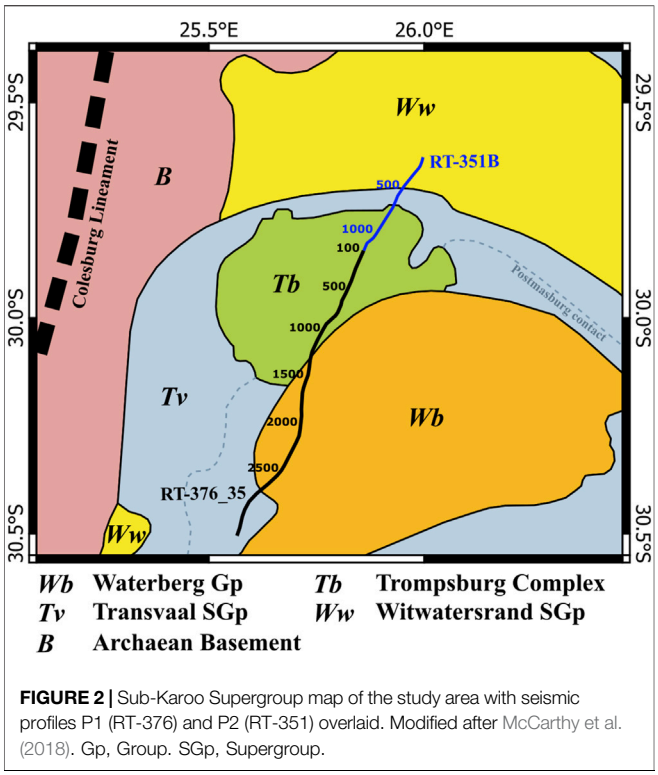

FIGURE 2 | Sub-Karoo Supergroup map of the study area with seismic profiles P1 (RT-376) and P2 (RT-351) overlaid. Modified after McCarthy et al. (2018). Gp, Group. SGp, Supergroup.

manifests as a 50-km-wide circular anomaly in both geophysical maps whose circumference intersects P1 at common midpoint (CMP) 2000 in the SW and P2 at CMP 760 in the NE. The magnetic map exhibits concentric arcs of high amplitudes in the NW that taper off in the NE and SW regions, and the overall magnetic signature of the complex is weaker in the SE.

The surface geological map in **Figure 1** consists entirely of ~360–145 Ma Karoo Supergroup rocks, which comprise basal tillite from the Carboniferous Dwyka Group, shale from the Permian Ecca Group, mudstone and sandstone from the Permian to Triassic Beaufort Group, and dolerites from the Karoo Dolerite Suite (KDS), which intruded the Karoo following crustal rupture around 182 Ma under an extensional regime. These dolerite dykes and sills permeate most of the Karoo Supergroup. They typically exhibit saucer-shape geometry and vary in size from a few centimeters to hundreds of meters thick (Coetzee and Kisters, 2016). Scheiber-Enslin et al. (2014; 2021) noted the effect of the KDS on the seismic imaging of structures located thereunder; in regions where dolerite sills were located, a lack of seismic illumination was observed in the traces within these regions. This lack of illumination is likely due to a strong reflection coefficient along the boundary of the weathered overburden and the high-density sills (Elde et al., 2018; Scheiber-Enslin et al., 2021). The seismic profiles traverse exclusively the sandstones from the Adelaide Subgroup of the Beaufort Group, as well as various dolerite outcrops from the KDS.

Due to lack of outcrop as well as ~1.5 km thick Karoo cover, mapping of sub-Karoo geology in the Trompsburg area has been inferred primarily from geophysical maps and boreholes (Borchers, 1964; Stratten, 1970; Pretorius, 1986; McCarthy et al., 2018). A sub-Karoo map of the southern Kaapvaal Craton was created by McCarthy et al. (2018) that details proposed extents of sub-Karoo lithologies with varying degrees of confidence. In their analysis, 22 boreholes were used to construct the sub-Karoo map in the region of the Trompsburg Complex. A simplified version of this map is shown in **Figure 2** with seismic profiles P1 and P2 overlaid.

Lying on the Archaean granite basement are quartzites, shales and diamictites that were intersected by boreholes to the east and NE of the Trompsburg Complex. Based on borehole correlations and zircon dating of the core samples, McCarthy et al. (2018) interpreted these as belonging to the West Rand and Central Rand Groups of the Archaean Witwatersrand Supergroup (2.9–2.7 Ga), which collectively compose the Colesburg Basin in the study area.

Sandwiched between the Witwatersrand and overlying rocks are the basalts and more localized quartzites and mafic units that comprise the late Archaean Ventersdorp Supergroup in the study region. McCarthy et al. (2018) note that these predominantly basaltic rocks underlie most of the Transvaal Supergroup across the Kaapvaal Craton and are present in boreholes ~50 km SW of the centre of the Trompsburg complex, just off the southernmost extent of seismic profile P1. According to the pre-Karoo map in **Figure 2**, the Ventersdorp rocks do not subcrop against the Karoo cover. They are thus expected to pinch out somewhere along the traverse of the seismic profiles before the Witwatersrand metasediments subcrop near the NE end of the profile (**Figure 2**).

The Neoarchaean-Paleoproterozoic Transvaal Supergroup (2.65–2.05 Ga) overlies the Witwatersrand and Ventersdorp Supergroups. In our study area, the Supergroup is confirmed by boreholes to be composed of dolomites and BIFs of the Chuniespoort Group, and basalts of the Pretoria Group. Two of the outer boreholes drilled into the Trompsburg geophysical anomaly intersected dolomites that Ortlepp (1959) first interpreted as belonging to the Transvaal Supergroup, which is now generally accepted. McCarthy et al. (2018) note that the BIFs are responsible for a strong v-shaped magnetic signature south of Trompsburg and infer from the anomaly shape that these formations are part of a NE plunging syncline.

The only pre-Karoo stratigraphic units observed in the area that are potentially younger than the 1915 ± 6 Ma Trompsburg Complex belong to what McCarthy et al. (2018) generically related to the Paleoproterozoic Waterberg Group (~2–1.8 Ga). This interpretation needs to be revisited considering recent work by Van Niekerk and Beukes (2019) on the Kheis Supergroup, a Waterberg equivalent with regional extent in the Northern Cape, far closer to the study area than the latter basin situated in the Limpopo Province. The oldest age obtained from the Hartley Formation, near the base of Kheis Supergroup is 1915.6 ± 1.4 Ma (Van Niekerk and Beukes, 2019), coinciding within error with the age of the underlying Trompsburg intrusion. Red arenites which exhibited similar composition and ages to those found in the Kheis Supergroup/Waterberg group were intersected by boreholes SE of the complex, implying the presence of an outlier of the basin in the vicinity of the complex (McCarthy et al., 2018). While Buchmann (1960) attributed the weak

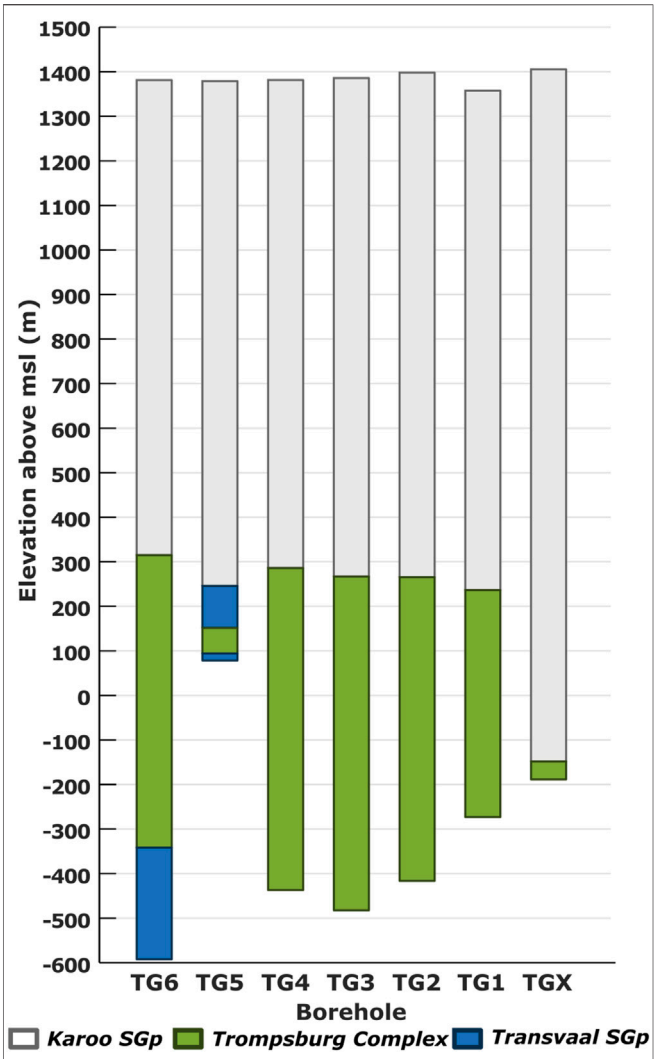

FIGURE 3 | Summary of cores of boreholes TG1 through TGX. Locations of boreholes can be seen in **Figure 1**.

geophysical signal in the SE portion of the Trompsburg Complex (**Figure 1**) to a lack of crystalline limestone within the Transvaal metasediments and thicker Karoo cover, McCarthy et al. (2018) suggested that the complex is overlain by Waterberg sediments (**Figure 2**) in this region, resulting in a weaker geophysical signature.

GEOLOGY OF TROMPSBURG COMPLEX

Boreholes

Logs of the boreholes that were drilled into the Trompsburg Complex in the 1950s are summarized in **Figure 3**. A more detailed log of the lithostratigraphy can be found in Ortlepp (1959) and Buchmann (1960). Holes TG1 through TG6 are located within the NW extents of the complex while hole TGX is located 200 m off the centre of the two seismic profiles (**Figure 1**). Each of the former six boreholes intersected mafic to ultramafic units belonging to the Trompsburg Complex, which are mostly gabbroic with intermittent magnetite, troctolite and anorthosite. The gabbro is dominated by plagioclase and olivine, and includes intermittent samples of clino-pyroxene and ortho-pyroxene. The two outermost boreholes (TG5 and TG6) contained samples of marble from the Transvaal Supergroup into which the complex intruded (Maier et al., 2003). The only igneous rock belonging to the complex that was interested by, and

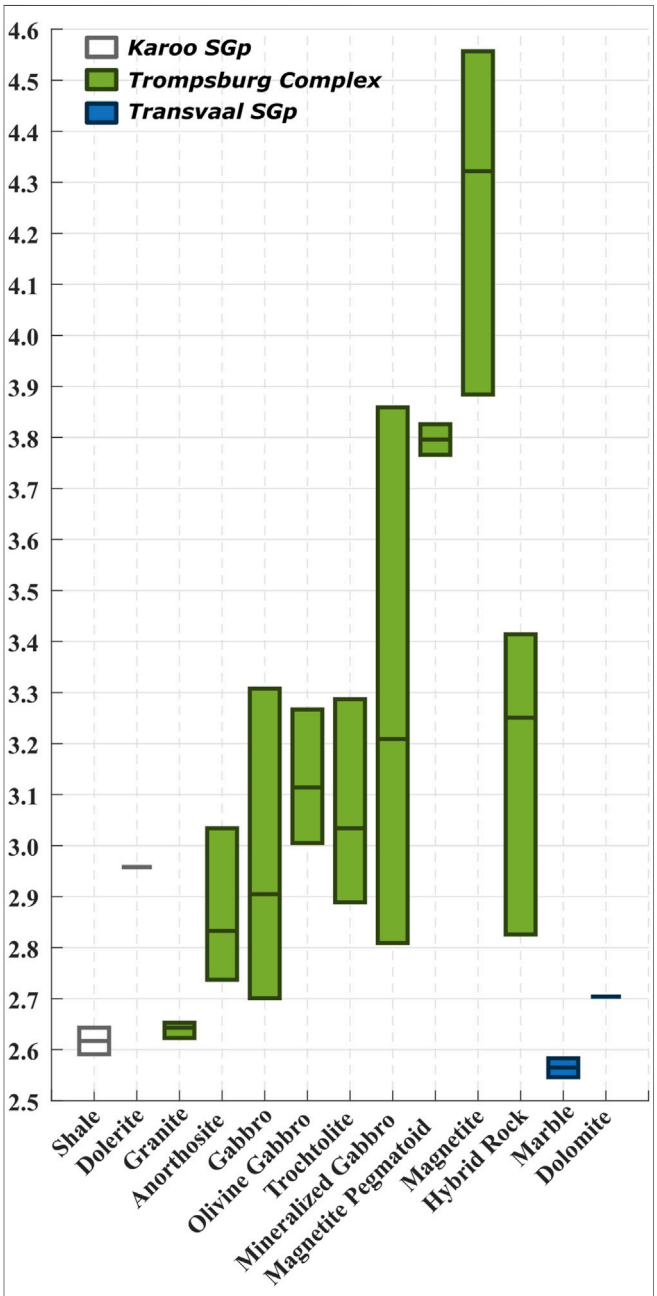

FIGURE 4 | Summary of density measurements of lithologies identified by Maré and Cole (2006). Bar limits denote maximum and minimum density values and centre lines denote average density values. Note that only one measurement was made on dolerite and dolomite samples.

found exclusively in, borehole TGX was a course-grained granophyric granite containing quartz, orthoclase and oligoclase grains (Ortlepp 1959).

Karoo sediments in each of the boreholes exhibit composite thicknesses of 1,558 m near the centre of the Trompsburg complex (borehole TGX), and 1,051–1,137 m near the outer rim of the complex (boreholes TG1 to TG6). As the latter six boreholes are clustered in the NW region of the complex and TGX located approximately 14 km to the SE, an explanation for the change in thickness is mostly conjectural. Ortlepp (1959) attributes the change in thickness either to a gentle NW-SE dip of the sub-Karoo topography, in which the sediment package was tilted prior to erosion, or a local valley/depression prior to deposition of the Karoo sediments. McCarthy et al. (2018) record Karoo thicknesses equal to those of TGX in boreholes located 33 km northeast, and 35 km south, of TGX.

Buchmann's (1960) interpretation of the boreholes and geophysical maps consisted of a gently NW-SE dipping Karoo cover, which overlie Trompsburg intrusions. The latter are characterized in the NW by gabbro and anorthosite layers with a 30° dip towards the centre of the intrusion, where granitic intrusions dominate the complex, reaching depths of 11 km.

Physical Properties

The 3D model of the Trompsburg Complex produced by Maré and Cole (2006) is based on physical property measurements on core retrieved from the TG1-TGX boreholes. The authors categorized samples of the cores, based primarily on their physical property contrasts and informed by the principal rock types logged by Ortlepp (1959), into quasilithological units (that is, representative units grouped by physical properties without further distinction).

Included in the physical property measurements made by Maré and Cole (2006) were density measurements, which are summarized in **Figure 4**. Due to lack of sonic measurements within the boreholes, acoustic impedance calculations, and therefore reflectivity modelling, is not possible. However, the density measurements can serve as first-order proxies of the reflectivity along boundaries between the quasilithological units. This can aid in a cautious interpretation of the reflection seismic profiles.

The relatively lower density values are attributed to shales from the Karoo Supergroup (2.61 g/cm^3) as well as marble and dolomites from the Transvaal Supergroup (2.56 g/cm^3 and 2.7 g/cm^3 respectively), which are substantially less dense than those of the Trompsburg intrusive rocks. Other than the 2.62 g/cm^3 granite, the rocks belonging to the Trompsburg complex exhibit densities much higher than the surrounding units, with values ranging from 2.7 to 4.5 g/cm^3. Within the Trompsburg suite, magnetite exhibits the highest average density of 4.32 g/cm^3 (**Figure 4**).

While these values do not give a direct measure of the seismic reflectivity in the region, it is useful to note the most significant density contrasts serve to inform the interpretation of the seismic profile rather than to serve as a basis thereof. Where the Karoo shales overlie the mafic components of the Trompsburg complex, there is a strong density contrast averaging 0.69 g/cm^3. A significant density contrast of 0.3 g/cm^3 occurs between Karoo shales and Karoo dolerites. However, a less significant contrast is found between the densities of the Karoo shales and the Trompsburg granites (0.02 g/cm^3), the latter of which are present near the centre of the Trompsburg Complex within borehole TGX. A strong density contrast (0.6 g/cm^3) is also present between the Trompsburg igneous rocks and the Transvaal dolomites and marble. Within the Trompsburg units, magnetite samples exhibit significantly higher density values than the rest of the igneous rocks, which could be the source of reflections within the complex.

METHODOLOGY

Seismic Acquisition

Acquisition of seismic profiles P1 and P2 were commissioned separately by Anglo-American, the former in 1990 and the latter in 1991, and share mostly identical acquisition parameters, which are summarized in **Table 1**. Both profiles utilized four seismic vibrators in a linear array with a linear sweep of 10–61 Hz. Shot and receiver spacing for each profile were both 50 m. Each shot record of both profiles comprised a total of 120 channels in a split-spread geometry that spanned a total distance of 5,950 m. Sercel SM4U 10 Hz geophones were used for both profiles and the sampling rate for both was 4 ms, with a total record length of 6 s. The profiles were acquired end-to-end with a SSW-NNE bearing that traversed roads through the centre of the Trompsburg potential field anomaly (**Figure 1**), spanning a total distance of 110 km, with a 3 km overlap.

Seismic Processing

The full processing flow of the reflection seismic profiles is summarized in **Table 2**. After verifying and integrating the retrieved geometry with the seismic data, the prestack component of the processing was conducted. This comprised initial datum and refraction statics, followed by a spiking deconvolution and bandpass frequency filter (60–10–99–120 Hz). A frequency-wavenumber (*f-k*) filter was then applied to remove ground roll and low-velocity (<3,500 m/s) linear signals. Velocity analysis consisted of constant velocity stack analysis on every 50th CMP gather and accompanied with iterative residual static corrections. **Figure 5** illustrates the improvement in reflection signals via the pre-stack workflow (blue arrows), as well as the suppression of ground roll (orange arrows) and first break arrivals (red arrows). Finally, before conversion to the depth domain, a Kirchoff pre-stack time migration was conducted to place reflections in their correct orientation and to collapse diffractions associated with sharp velocity contrasts. Due to the lack of velocity logs or other constraining depth data, the conversion to depth was performed using a smoothed version of the RMS velocity model.

TABLE 1 | Acquisition parameters for profiles P1 and P2

Acquisition parameter	RT-376 (P1)	RT-351 (P2)
Shooting Direction	N-S	
Spread	Split spread: 2975m-25m-25m–2975m. 120 active channels	
Recording Instrument	Sercel SN368	
Geophones	Sercel SM4U 1C–10 Hz	
Receiver Spacing	50 m	
Sampling Interval	4 ms	
Source	4 vibs, 3 sweeps per vib point	
Sweep Parameters	10–61 Hz linear sweep	
Source Spacing	50 m	
Profile Length	80 km	30
Nominal Fold	60	

TABLE 2 | Processing flow of seismic profiles.

Processing Step	Parameters: RT-376 (P1)	Parameters: RT-351 (P2)
1. Geometry	Write geometry to SEGY headers	
2. CMP binning	Crooked line. CMP bin spacing: 25 m	
3. Static corrections	Floating datum 1,550 m SRD 3,000 m/s rep. vel Refraction Statics: 6.2 ms RMS	Floating Datum 1,475 m SRD 3,000 m/s rep. vel Refraction Statics: 8.8 ms RMS
4. Deconvolution	Spiking deconvolution	
5. Frequency filter	Bandpass: 6–10–99–120 Hz	
6. F-K filter	Mute signals with velocities <3,500 m/s	
7. Velocity Analysis	Constant velocity stack analysis every 50th CMP	
8. Residual statics	4 iterations	
9. Migration	2D Kirchoff pre-stack time migration	
10. Stack	Normalized stacking	
11. Frequency filter	Bandpass: 10–18–50–70 Hz	
12. Depth conversion	Time-to-depth conversion using smoothed interval velocity model	

RESULTS

The final migrated and depth-converted seismic sections, along with CMP fold plots and potential field plots, for profiles P1 and P2 are shown in **Figures 6A,B**, respectively. CMP labels of the sections decrease from left to right in **Figure 6** because acquisition of the profiles was from NE to SW. Presented here are the observed seismic facies and boundaries.

A first glance at **Figures 6A,B** reveals that a significant amount of the seismic energy is contained within the top half of the sections. In particular, most of the high-amplitude reflections are restricted to the top 2 km of both sections. Lying beneath these is a reflection package that is present throughout both profiles at a constant 0 m-above-sea-level (msl), which is labelled R1 in **Figures 6B,C**. R1 has a high amplitude, with exception to areas of low fold such as at CMPs 2,700 and 1,000 of P1, as well as a distinctive reflectivity reminiscent of bedding.

Beneath R1, between CMPs 2000 and 1,200 of P1, is another strong reflection with a 30° dip to the SW. This reflector bears similar seismic reflectivity and (reverse) dip to a reflector located between CMPs 3,000 and 2,200 of P1. These reflectors, collectively labelled R2 in **Figure 6**, trace out a concave bowl beneath R1 with a discontinuous apex at CMP 2250 and elevation -2,500 msl. The discontinuity displaces the SW R2 reflector about 500 m above the NE reflector and is interpreted as a reverse fault that extends into deeper units.

The region of the profiles where Trompsburg reflectors are expected is characterized by chaotic reflection zones and weak, discontinuous reflections (**Figure 6C**). The reflections can be

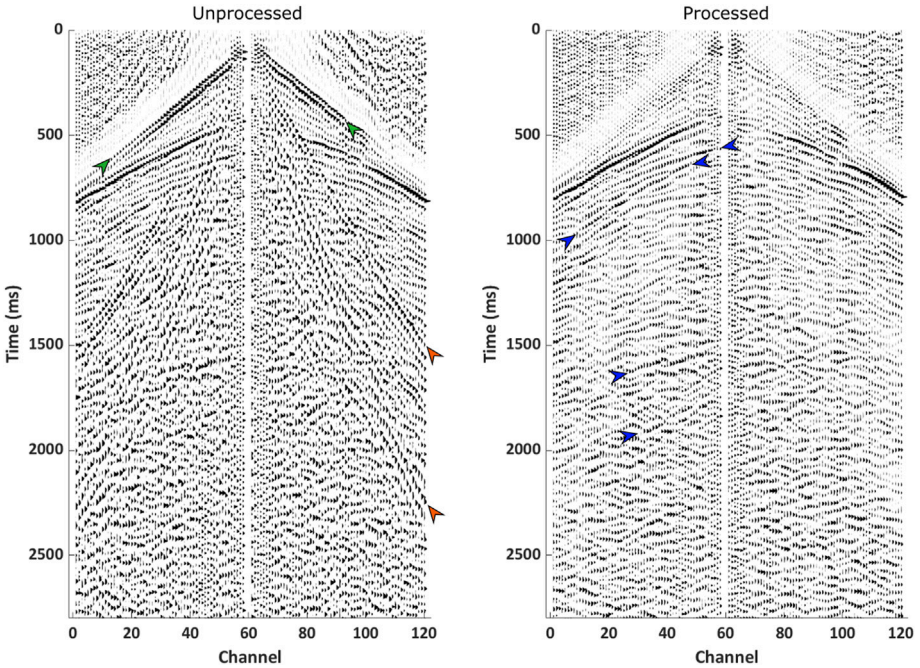

FIGURE 5 | Example shot gather from profile P1 (RT-376) before and after prestack processing flow. Green and orange arrows indicate first break and ground roll signals, respectively, that were removed. Blue arrows highlight enhanced reflection signals.

grouped by dip into three groups. The first group of reflections dip to the NE and are labelled R4. They lie between CMPs 2,200 and 1,100 of P1 and have a consistent dip of ~30°. The second group of reflections, labelled R5, has near-zero dip between CMPs 1700 and 1,000 and exhibits seismic facies characteristic of complex layering. The third group consists of reflections with a SW dip labelled R6. The R6 reflections have either a ~30° or a 45° dip; the former are observed closer to the centre of the expected complex and the latter along the NE bounds.

Approximately 1 km below and parallel to the SW R2 reflector is a more attenuated reflector labelled R3 (**Figure 6C**). Accompanying R3 is a weaker parallel reflector ~500 m below it. A series of weak, almost horizontal reflectors, labelled R8, are located beneath R3 at an elevation of -3,000 msl (**Figure 6C**). Two reflector packages labelled R9 and R10 in **Figures 6B,C** lie beneath R8. In profile P1 (**Figure 6C**), both R9 and R10 exhibit strong reflection amplitudes and appear to have a high degree of thrust-faulting.

Interpretation

In **Figures 6B,C**, strong reflections have been traced in black and interpreted stratigraphic units, as discussed in this section, have been overlaid on the migrated seismic sections of the respective profiles. While the focus of the seismic interpretation is on the Trompsburg Complex, first order interpretations of other supracrustals belonging to the Witwatersrand, Ventersdorp, Transvaal, Kheis, and Karoo Supergroups are given. Most of the seismic energy is concentrated in the top 2 km of the section, leaving less energy to transmit to deeper strata including the target Trompsburg Complex. Thus, our interpretations are informed largely by the *a priori* geophysical and geological datasets: magnetic, gravimetric, and geological maps, as well as the physical property data. The interpretation presented here provides, in our estimation, the model that best explains the combined set of these datasets with the observed seismic reflections.

Another factor that must be considered in the interpretation is that the depth conversion was performed using the RMS velocity model due to lack of constraining data in the area. This means that accuracy in depth is limited by the presence and accuracy in picked velocities. Where velocity picks were sparse, i.e., where there were no clear coherent reflection events, there is no strong tie between time and depth. Furthermore, any coherent events in time that are preceded by a gap in the velocity model are also limited in accuracy of depth. This makes it challenging to produce an accurate model in the depth domain. Despite these challenges, depth conversions based on picked velocities, or even with constant velocity models, have proven to be robust in multiple hardrock settings (e.g. Markovic et al., 2019; Westgate et al., 2020), and we are relying on this robustness in our interpretation.

The reflections in the top 2 km are due primarily to the dolerite suite within the Karoo cover. The characteristic saucer shape of the sills is evident throughout the Karoo in **Figures 6B,C**. We interpret the high-amplitude and bedding-like reflectivity of R2 as resulting from the basal Dwyka Group of the Karoo Supergroup. This interpretation is consistent with the density contrasts in **Figure 4**. With this interpretation, the average total thickness of the Karoo cover across the seismic profiles is 1,400 m, which correlates with observations from borehole TGX, located near

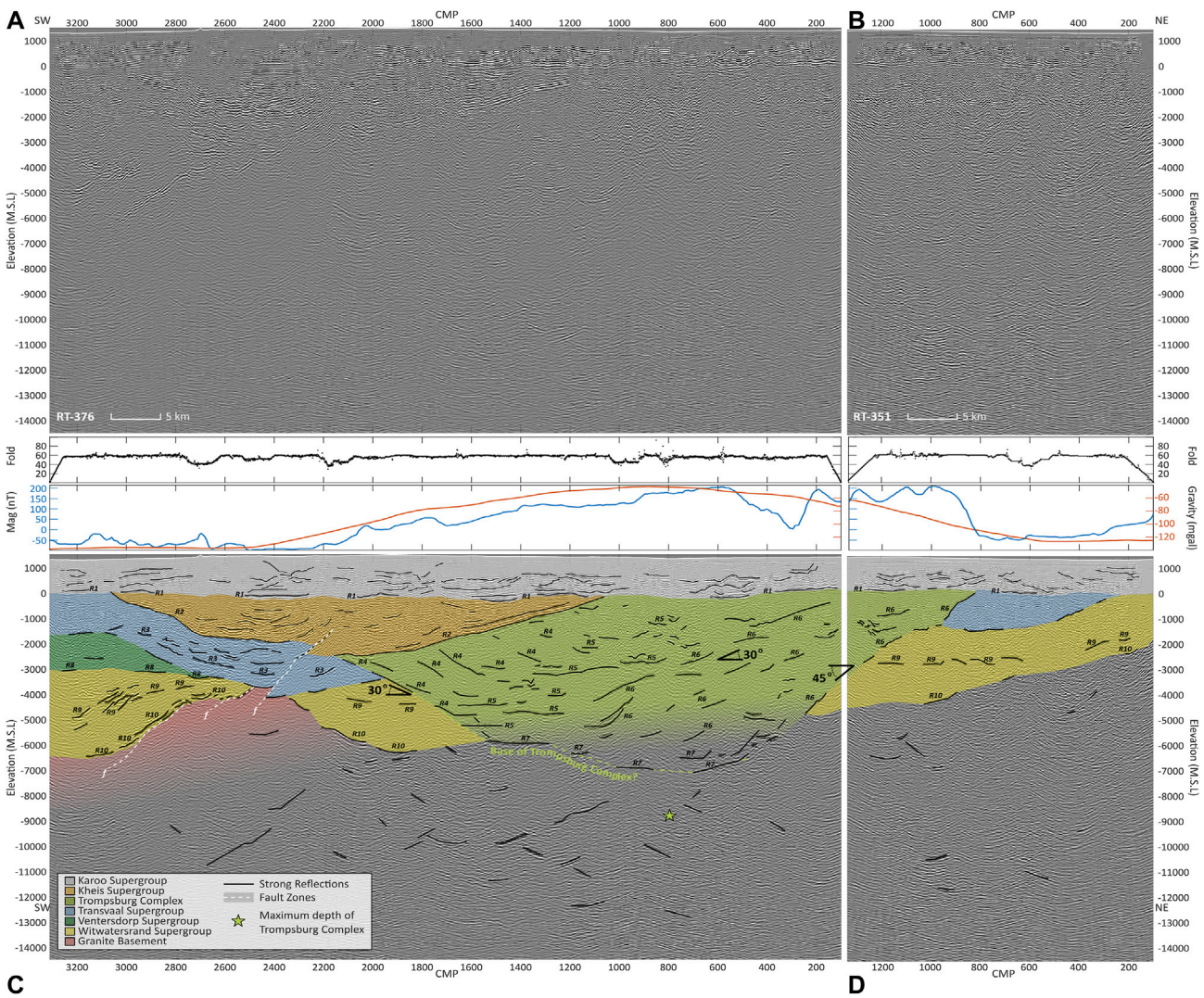

FIGURE 6 | Uninterpreted migrated sections of profiles P1 (RT-376; **A**) and P2 (RT-351; **B**) as well as fold plots, potential field plots, and interpreted sections **(C,D)**. Potential field data were obtained by sampling the relevant maps displayed in **Figure 1** along the seismic profiles. Interpreted sections comprise black lines denoting identified reflections, faults in dotted white lines, and stratigraphic units in colour. Identified reflectors are labelled as cited in the text.

CMP 900 of P1 (**Figure 6C**), as well as other boreholes in the region (McCarthy et al., 2018).

The R2 reflectors pinch out against the Karoo cover where P1 intersects the boundary of the Waterberg Group (i.e., Kheis Supergroup) in the pre-Karoo map by McCarthy et al. (2018) (**Figure 2**). The R2 reflectors are thus interpreted as the base of the Kheis Supergroup, which attains a maximum thickness at CMP 2200 of 2.5 km, and has a total lateral sub-Karoo expanse of 45 km along the traverse of P1.

R4 and R6 are interpreted as comprising the SW and NE boundaries of the Trompsburg Complex, respectively. With this interpretation, the total sub-Karoo expanse of the complex along the profiles is 60 km. The SW third of the complex is overlain by Kheis Supergroup sediments and the NE boundary of the Trompsburg Complex is located beneath the Karoo cover near CMP 800 of P2. Both of these observations are consistent with the geophysical maps in **Figure 1** and the pre-Karoo map in **Figure 2**. The potential field plots in **Figure 6** reinforce this interpretation: maximum values in both magnetic and gravity data are located above the R5 reflectors, centred between the R4 and R6 pinch-outs. Additionally, the potential field profiles both exhibit, especially the magnetic profile, a more gradual increase of amplitude in the SW approaching the centre of the interpreted complex, and a rapid decrease in the NE. The gradual SW limb can be explained by the overlying Kheis rocks and a 30° dip of the Trompsburg intrusions, while a steeper 45° dip and no overlying rocks beneath the Karoo yield a steeper NE potential field limb. The magnetic data exhibits short wavelength (~5 km) amplitude fluctuations near the overlap region of the two profiles. We interpret this as intermittent mineralization within the Trompsburg Complex. The lack of

strong and coherent reflections below −5,000 msl obscures distinction between Trompsburg-related reflections and basement reflections, resulting in an unconstrained basal reflection of the complex. A series of weak reflections at about −7,000 msl, labelled R7, are tentatively interpreted as the base of the complex, rendering it with a maximum thickness of ~6.6 km.

The R3 reflector is interpreted to be from iron mineralization within the BIFs of the Chuniespoort Group of the Transvaal Supergroup. Its fluctuating amplitude could be resultant of varying degrees of mineralization density along the horizon. The underlying weaker reflector is interpreted as the quartzites that comprise the base of the Transvaal metasediments (McCarthy et al., 2018). Between CMPs 2,400 and 2,200 (**Figure 6C**) the metasediments are disrupted by the aforementioned reverse fault that displaced the base of the Kheis Supergroup, before they pinch out against the boundary of the Trompsburg Complex. In profile P2 (**Figure 6D**), the Transvaal Supergroup is interpreted to lie NE of the Trompsburg Complex with a thickness of 1 km, which tapers off at CMP 250.

R8 is interpreted as the base of the Ventersdorp Supergoup, which averages in thickness of 1.2 km and pinches out beneath the Transvaal metasediments near CMP 2600. This interpretation is consistent with boreholes lying ~50 km SW of the town of Trompsburg as detailed by McCarthy et al. (2018).

R10 is interpreted as the base of the Witwatersrand Supergroup and R9 as an internal reflection, likely associated with the base of the Central Rand Group. R10 pinches out against the Transvaal Supergroup at CMP 2500 of P1 due to a reverse fault that terminates at the base of the Transvaal Supergroup and is subparallel to the aforementioned reverse fault that extends into the Kheis. The Witwatersrand strata are interpreted to reemerge near CMP 2300 and extend further NE until being truncated by the Trompsburg Complex. On the NE side of the complex, the Witwatersrand rocks directly underlie the Transvaal metasediments before subcroping against the Karoo Supergroup at CMP 220 in P2.

The basement, which is interpreted to exist at depths greater than 6 km, exhibits a collection of both discontinuous reflections with randomly distributed orientations and migration "smile" signals. These could be computational artefacts caused by the migration or related to changes in the basement facies (such as localized metamorphism, for example).

DISCUSSION AND CONCLUSION

Certainty in the geological interpretation of seismic data is reduced when dealing with 2D data. True dips and thicknesses cannot be determined from a 2D section and out-of-plane reflections can lead to misinterpretations of in-plane features. This is exacerbated by implications of the hardrock setting and layered igneous plumbing systems: seismic energy that is scattered ubiquitously due to heterogeneities in rock characteristics, and complex subsurface structures as the result of metamorphism, all lead to a complex wavefield and seismic reflections that have weak amplitudes and coherence across traces. Seismic interpretation is non-unique and there can be multiple plausible geological models that fit the same seismic data, especially if it is 2D. The interpretation we present in **Figures 6C,D** is based to a large degree on the constraining datasets (magnetic, gravimetric and geological maps, as well as the borehole and physical property measurements).

In addition to these factors, as is the case with seismic profiles P1 and P2, the surficial Karoo Supergroup is laden with dolerite intrusions. The large acoustic impedance contrast along the boundaries between the igneous dolerites and the Karoo sediments causes scattering of seismic energy and diminishes transmission of seismic energy to deeper layers. This is a common obstacle in the reflection seismic method (e.g., Eide et al., 2018; Scheiber-Enslin et al., 2021). There are thus varying degrees of confidence in the interpreted units laid out in **Figures 6C,D**, with the highest confidence placed on the interpretations pertaining to the Karoo Supergroup and Kheis Supergroup. Interpretations of the other supracrustal units, including the Trompsburg Complex, rely heavily on the supporting literature mentioned in earlier chapters (Ortlepp, 1959; Buchmann, 1960; McCarthy et al., 2018).

Seismic interval velocities within the two profiles range from 4,000 m/s to 6,500 m/s, with the former being attributed to Karoo sediments and the latter to metamorphosed basement granite. These velocities coincide with those recorded in the literature (Stettler et al., 1999; Tinker et al., 2002; Durrheim, 2015). The average seismic velocity of the sub-Karoo seismic waves was 5,000 m/s and the dominant frequency of the migrated data is 30 Hz. Using the Widess quarter-wavelength criterion (Widess, 1973), the vertical seismic resolution is thus 40 m. Our first order interpretation of sub-Karoo supracrustals requires a significantly less stringent resolution limit. Upon migration, this is also the horizontal resolution of the seismic data (Yilmaz, 2001).

The centre of the Trompsburg geophysical anomaly (**Figure 1**) is located near CMP 1000 of profile P1, and tapers off near CMP 2000 of P1 to the SW, and CMP 1000 of P2 to the NE. The bounds of the seismically interpreted Trompsburg Complex (**Figure 6**) correlate well with these locations. Borehole TGX, located near CMP 900, intersected Trompsburg granite at an elevation of −150 msl (**Figure 3**), which is the same elevation that the complex subcrops against the Karoo in our model (**Figure 6**). Additionally, our model conforms with the interpretation by McCarthy et al. (2018) that the weaker potential field signature of the Trompsburg Complex in its southern region is attributed to overlying sediments from the Kheis Supergroup. The Kheis Supergroup in **Figure 6C** lies within the bounds interpreted by McCarthy et al. (2018) in their sub-Karoo map (**Figure 2**), with a maximum thickness of 2.5 km. Furthermore, the 30° dip of the Trompsburg layers in the outer SW and inner NE sections of our interpretation is the same as the dip that Buchmann (1960) characterized for the NW outer Trompsburg layers based on the boreholes drilled in the 1950s. Hence, our seismic interpretation of the Trompsburg Complex is fairly well constrained by previous studies in the literature.

While multiple reflectors were identified within the Trompsburg Complex, their lack of continuity, complex layering reflection patterns, and weak reflection amplitude

prevented distinction between internal layers within the complex. The absence of strong reflections within the complex can be attributed to a general lack of seismic energy penetrating beneath the Karoo, or an insignificant acoustic impedance contrast. The densities illustrated in **Figure 4** suggest that any significant reflections originating from within the complex would be associated with zones of mineralization; it is possible that mineralization within the complex is restricted to the NW and N regions. The seismic profiles appear to traverse a break in the magnetic high along the outer rim of the complex (**Figure 1**).

The 6.6 km thickness of the Trompsburg Complex near its centre at CMP 800 (**Figure 6**) is more partial to Buchmann's (1960) 10 km thickness than to Ortlepp's (1959) 2–3 km. The 3D potential field model by Maré and Cole (2006) required a centre thickness of 16 km (6 km without the modelled feeder, which is the closest value to the seismic thickness). While the 6.6 km central depth of the complex in **Figure 6** is not tightly substantiated, a further constraint can be placed on the basal depth of the complex by extending the 30° dipping SW bound of the complex and the 45° dipping NE bound of the complex and finding their intersection. Whilst this gives a reasonable depth constraint, it is possible that reflectors with dips greater than 45° are less likely to be imaged, hence the depth obtained by this method is essentially a minimum depth. The result is marked with a green star in **Figures 6C,D** is located at CMP 800 and −9,000 msl, which corresponds to a maximum thickness of 7.5 km for the complex. At this point, no strong or continuous reflections can be associated with the base of the complex, nor with the contact between mafic rocks and the central granite.

Apart from the Trompsburg and Kheis rocks, the pre-Karoo supracrustals that were identified in the seismic profiles with a moderate degree of certainty were the Witwatersrand, Ventersdorp, and Transvaal Supergroups. The Ventersdorp Supergoup exhibits a maximum thickness of 1.1 km at the SW end of profile P1 and pinches out between the other two aforementioned units before they are intruded by the Trompsburg Complex. The Witwatersrand Supergroup is discontinuous in the SW portion of the seismic profiles due to reverse and thrust faulting, and is continuous NE of the Trompsburg intrusion with an average thickness of 2 km. The Transvaal Supergroup underlies the Kheis Supergroup in the SW before it is intruded by Trompsburg rocks. It is faulted in this region and has an average thickness of 1.5 km. NE of the Trompsburg Complex, the Transvaal Supergroup has a thickness of 1 km before pinching out further NE, where Witwatersrand Supergroup subcrops against the Karoo cover. The basement boundary is uncertain throughout much of the profiles due to the lack of reflections associated therewith, and the seismic signature at >7 km depths is chaotic and incoherent.

In summary, our interpretation of the seismic profiles P1 and P2 suggests that the Trompsburg Complex is ~6.6 km thick near its centre, has a 60 km lateral extent beneath the Karoo cover, and is overlain by Kheis Supergroup sediments in the SE. Due to weak seismic energy at depth, intra-Trompsburg layering was not resolvable but dips of various reflectors within the complex were identified to be 30° near its SW extent, and 45° near its NE extent, where the complex intruded into supracrustals comprising both Witwatersrand and Transvaal Supergroups. Lastly, the reverse fault at CMP 2400 and the broad synform structure of the Kheis and Transvaal Supergroups between CMP 3000 and CMP 1000 appear consistent with the thrusting style of deformation characteristic of the Kheis Supergroup (Van Niekerk and Beukes, 2019).

We have shown in this study that integration of seismic reflection data with geological and potential field data is useful in constraining the expanse and depth of the Trompsburg Igneous Complex. In general, the seismic method is an important tool in discovering and characterizing igneous plumbing systems and possibly unlocking the economic potential thereof. 3D seismic surveys in particular are not restricted by the challenges that come with 2D data, such as dip and thickness approximations, out-of-plane anomalies, inaccuracies in migration imaging, etc. Layered intrusions often exhibit strong acoustic impedance contrasts, both internal (due to mineralization zones as well as density contrasts between subsequent intrusion events) and external (due to strong density contrasts between igneous intrusions and sedimentary host rocks as well as metamorphism thereby) that allow for the detection and resolution of such boundaries (e.g., Deemer and Huricj, 1997; Manzi et al., 2019; Sehoole et al., 2020).

DATA AVAILABILITY STATEMENT

The original contributions presented in the study are included in the article/Supplementary Material, further inquiries can be directed to the corresponding author.

AUTHOR CONTRIBUTIONS

MW was responsible for processing and interpreting the seismic data, as well as drafting the manuscript and assembling all images. MM conceptualized the research project, facilitated the seismic data transfer and assisted with seismic interpretation and manuscript writeup. IJ assisted with seismic data processing. MA assisted with interpretation of structural geology within seismic data. RD assisted with seismic processing and interpretation.

FUNDING

This project was funded by CIMERA. The support of the DSI-NRF Centre of Excellence (CoE) for Integrated Mineral and Energy Resource Analysis (DSI-NRF CIMERA) towards this research is hereby acknowledged. Opinions expressed and conclusions arrived at are those of the authors and are not necessarily to be attributed to the CoE.

ACKNOWLEDGMENTS

In addition to the CoE who funded this project, the donation of seismic data by AngloGold Ashanti is acknowledged and greatly appreciated. HiSeis Pty. Ltd. is acknowledged for sponsoring Petrosys Globe Claritas software licenses that

enabled processing of the seismic data. The Council of Geosciences of South Africa is also acknowledged for providing geological, gravity magnetic data. The work presented here was facilitated by the Seismic Research Centre at the University of the Witwatersrand, South Africa, without which this research would not have been possible.

REFERENCES

Borchers, R. (1964). "Exploration of the Witwatersrand and its Extensions," in *The Geology of Some Ore Deposits in Southern Africa*. Editor S. H. Haughton (Johannesburg, South Africa: Geological Society of South Africa), 1–24.

Buchmann, J. P. (1960). Exploration of a Geophysical Anomaly at Trompsburg, Orange Free State, South Africa. *Trans. Geol. Soc. South Africa* 63, 1–10.

Buick, I. S., Maas, R., and Gibson, R. (2001). Precise U-Pb Titanite Age Constraints on the Emplacement of the Bushveld Complex, South Africa. *J. Geol. Soc.* 158 (1), 3–6. doi:10.1144/jgs.158.1.3

Buske, S., Bellefleur, G., and Malehmir, A. (2015). Introduction to Special Issue on "Hard Rock Seismic Imaging". *Geophys. Prospecting* 63 (4), 751–753. doi:10.1111/1365-2478.12257

Coetzee, A., and Kisters, A. (2016). The 3D Geometry of Regional-Scale Dolerite Saucer Complexes and Their Feeders in the Secunda Complex, Karoo Basin. *J. Volcanology Geothermal Res.* 317, 66–79. doi:10.1016/j.jvolgeores.2016.04.001

Deemer, S., and Hurich, C. (1997). Seismic Image of the Basal Portion of the Bjerkreim-Sokndal Layered Intrusion. *Geol* 25 (12), 1107–1110. doi:10.1130/0091-7613(1997)025<1107:siotbp>2.3.co;2

Durrheim, R. J. (2015). "Structural Seismology: Investigations of the Crust and Mantle," in *The History of Geophysics in Southern Africa*. Editor J. H. de Beer (Stellenbosch, South Africa: Sun Press), 165–189.

Eide, C. H., Schofield, N., Lecomte, I., Buckley, S. J., and Howell, J. A. (2018). Seismic Interpretation of Sill Complexes in Sedimentary Basins: Implications for the Sub-sill Imaging Problem. *J. Geol. Soc.* 175 (2), 193–209. doi:10.1144/jgs2017-096

Logan, C. T. (19792012). A Mineralogical Investigation of Borehole Cores from the Trompsburg Complex. *MINTEK. Rep. no.*, 1–16.

Maier, W. D., Peltonen, P., Grantham, G., and Mänttäri, I. (2003). A New 1.9 Ga Age for the Trompsburg Intrusion, South Africa. *Earth Planet. Sci. Lett.* 212, 351–360. doi:10.1016/s0012-821x(03)00281-4

Malehmir, A., Markovic, M., Marsden, P., Gil, A., Buske, S., Sito, L., et al. (2021). Sparse 3D Reflection Seismic Survey for Deep-Targeting Iron Oxide Deposits and Their Host Rocks, Ludvika Mines, Sweden. *Solid Earth* 12 (2), 483–502. doi:10.5194/se-12-483-2021

Manzi, M. S. D., Cooper, G. R. J., Malehmir, A., and Durrheim, R. J. (2019). Improved Structural Interpretation of Legacy 3D Seismic Data from Karee Platinum Mine (South Africa) through the Application of Novel Seismic Attributes. *Geophys. Prospecting* 68 (1), 145–163. doi:10.1111/1365-2478.12900

Maré, L. P., and Cole, J. (2006). The Trompsburg Complex, South Africa: A Preliminary Three Dimensional Model. *J. Afr. Earth Sci.* 44, 314–330. doi:10.1016/j.jafrearsci.2005.11.026

Markovic, M., Maries, G., Malehmir, A., Ketelhodt, J., Bäckström, E., Schön, M., et al. (2019). Deep Reflection Seismic Imaging of Iron-oxide Deposits in the Ludvika Mining Area of central Sweden. *Geophys. Prospecting* 68 (1), 7–23. doi:10.1111/1365-2478.12855

McCarthy, T. S., Corner, B., Lombard, H., Beukes, N. J., Armstrong, R. A., and Cawthorn, R. G. (2018). The Pre-karoo Geology of the Southern Portion of the Kaapvaal Craton, South Africa. *South. Afr. J. Geology.* 121 (1), 1–22. doi:10.25131/sajg.121.0006

Ortlepp, R. J. (1959). A Pre-karoo Igneous Complex at Trompsburg, Orange Free State, Revealed by Drilling Exploration. *Trans. Geol. Soc. South Africa* 62, 33–57.

Pretorius, C. C., Muller, M. R., Larroque, M., and Wilkins, C. (2003). "A Review of 16 Years of Hardrock Seismics on the Kaapvaal Craton," in *Hardrock Seismic Exploration*. Editors D. W. Eaton, B. Milkereit, and M. H. Salisbury (Tulsa, OK: Society of Exploration Geophysicists).

Pretorius, D. A. (1986). "The Witwatersrand Basin," in *Mineral Deposits of Southern Africa*. Editors C. R. Anhaeusser and S. Maske (Johannesburg, South Africa: Geological Society of South Africa).

Reynolds, I. M. (19792017). Vanadium-bearing Titaniferous Iron Ores from the Rooiwater, Usushwana, Mambula, Kaffirskraal, and Trompsburg Igneous Complexes. *MINTEK. Rep. no.*, 1–65.

Scheiber-Enslin, S. E., and Manzi, M. (2018). Integration of 3D Reflection Seismics and Magnetic Data for Deep Platinum Mine Planning and Risk Mitigation: a Case Study from Bushveld Complex, South Africa. *Exploration Geophys.* 49 (6), 928–939. doi:10.1071/eg17083

Scheiber-Enslin, S. E., Manzi, M., and Webb, S. J. (2021). Seismic Imaging of Dolerite Sills and Volcanic Vents in the Central Karoo, South Africa: Implications for Shale Gas Potential. *South. Afr. J. Geology.* 124 (2), 465–480. doi:10.25131/sajg.124.0043

Scheiber-Enslin, S. E., Webb, S. J., and Ebbing, J. (2014). Geophysically Plumbing the Main Karoo Basin, South Africa. *South. Afr. J. Geology.* 117 (2), 275–300. doi:10.2113/gssajg.117.2.275

Sehoole, L., Manzi, M. S. D., Zhang, S. E., and Bourdeau, J. E. (2020). An Innovative Seismic and Statistical Approach to Understand 3D Magmatic Structures and Ore Deposits in the Western Bushveld Complex, South Africa. *Ore Geology. Rev.* 126, 103784. doi:10.1016/j.oregeorev.2020.103784

Stettler, E. H., Prinsloo, J., Hauger, M. E., and du Toit, M. C. (1999). A Crustal Geophysical Model for the Kheis Tectonic Province, South Africa, Based on Magnetotelluric, Reflection Seismic, Gravity and Magnetic Data Sets. *South. Afr. Geophys. Rev.* 3, 54–68.

Stratton, T. (1970). "Sub-Karoo Geology of the Karoo Basin in South Africa," in Proceedings and Papers of the Second Gondwana Symposium (South Africa, 209–211.

Tinker, J., de Wit, M., and Grotzinger, J. (2002). Seismic Stratigraphic Constraints on Neoarchean - Paleoproterozoic Evolution of the Western Margin of the Kaapvaal Craton, South Africa. *South. Afr. J. Geology.* 105, 107–134. doi:10.2113/105.2.107

Van Niekerk, H. S., and Beukes, N. J. (2019). Revised Definition/outline of the Kheis Terrane along the Western Margin of the Kaapvaal Craton and Lithostratigraphy of the Newly Proposed Kheis Supergroup. *South. Afr. J. Geology.* 122 (2), 187–220. doi:10.25131/sajg.122.0014

Walraven, F., and Hattingh, E. (1993). Geochronology of the Nebo Granite, Bushveld Complex. *South. Afr. J. Geology.* 96, 31–41.

Westgate, M., Manzi, M. S. D., James, I., and Harrison, W. (2020). New Insights from Legacy Seismic Data: Reprocessing of Legacy 2D Seismic Data for Imaging of Iron-oxide Mineralization Near Sishen Mine, South Africa. *Geophys. Prospecting* 68 (7), 2119–2140. doi:10.1111/1365-2478.12996

Westgate, M., Manzi, M. S. D., Malehmir, A., Gibson, R. L., Andreoli, M. A. G., and Bumby, A. (2021). A Reappraisal of Legacy Reflection Seismic Data from the Western Margin of the Kaapvaal Craton, South Africa, with Implications for Mesozoic-Cenozoic Regional Tectonics. *Tectonophysics* 813, 228934. doi:10.1016/j.tecto.2021.228934

Widess, M. B. (1973). How Thin Is a Thin Bed? *Geophysics* 38 (6), 1176–1180. doi:10.1190/1.1440403

Yilmaz, O. (2001). Seismic Data Analysis: Processing, Inversion and Interpretation of Seismic Data. *Soc. Explor. Geophys.* 1, 1803–1805. doi:10.1190/1.9781560801580

Conflict of Interest: At the time of research/writing, Author IJ was employed by HighSeis Pty Ltd. They are now employed by Southern Geoscience Consultants.

The remaining authors declare that the research was conducted in the absence of any commercial or financial relationships that could be construed as a potential conflict of interest.

Publisher's Note: All claims expressed in this article are solely those of the authors and do not necessarily represent those of their affiliated organizations, or those of the publisher, the editors, and the reviewers. Any product that may be evaluated in this article, or claim that may be made by its manufacturer, is not guaranteed or endorsed by the publisher.